Journal of Bacteriology

Activity of the Osmotically Regulated *yqiHIK* Promoter from Bacillus subtilis Is Controlled at a Distance

Kathleen E. Fischer and Erhard Bremer

Updated information and services can be found at:
http://jb.asm.org/content/194/19/5197

These include:

SUPPLEMENTAL MATERIAL
http://jb.asm.org/content/suppl/2012/09/07/JB.01041-12.DCSupplemental.html

REFERENCES
This article cites 64 articles, 32 of which can be accessed free at: http://jb.asm.org/content/194/19/5197#ref-list-1

CONTENT ALERTS
Receive: RSS Feeds, eTOCs, free email alerts (when new articles cite this article), more»

Information about commercial reprint orders: http://journals.asm.org/site/misc/reprints.xhtml
To subscribe to to another ASM Journal go to: http://journals.asm.org/site/subscriptions/

Journals.ASM.org

Activity of the Osmotically Regulated *yqiHIK* Promoter from *Bacillus subtilis* Is Controlled at a Distance

Kathleen E. Fischer and Erhard Bremer

Philipps University Marburg, Department of Biology, Laboratory for Microbiology, Marburg, Germany

The *yqiHIK* gene cluster from *Bacillus subtilis* is predicted to encode an extracellular lipoprotein (YqiH), a secreted *N*-acetylmuramoyl-L-alanine amidase (YqiI), and a cytoplasmic glycerophosphodiester phosphodiesterase (YqiK). Reverse transcriptase PCR (RT-PCR) analysis showed that the *yqiHIK* genes are transcribed as an operon. Consistent with the *in silico* prediction, we found that the purified YqiI protein exhibited hydrolytic activity toward peptidoglycan sacculi. Transcription studies with *yqiH-treA* reporter fusion strains revealed that the expression of *yqiHIK* is subjected to finely tuned osmotic control, but enhanced expression occurs only in severely osmotically stressed cells. Primer extension analysis pinpointed the osmotically responsive *yqiHIK* promoter, and site-directed mutagenesis was employed to assess functionally important sequences required for promoter activity and osmotic control. Promoter variants with constitutive activity were isolated. A deletion analysis of the *yqiHIK* regulatory region showed that a 53-bp AT-rich DNA segment positioned 180 bp upstream of the −35 sequence is critical for the activity and osmotic regulation of the *yqiHIK* promoter. Hence, the expression of *yqiHIK* is subjected to genetic control at a distance. Upon the onset of growth of cells of the *B. subtilis* wild-type strain in high-salinity medium (1.2 M NaCl), we observed gross morphological deformations of cells that were then reversed to a rod-shaped morphology again when the cells had adjusted to the high-salinity environment. The products of the *yqiHIK* gene cluster were not critical for reestablishing rod-shaped morphology, but the deletion of this operon yielded a *B. subtilis* mutant impaired in growth in a defined minimal medium and at high salinity.

Most microorganisms possess turgor, an intracellular hydrostatic pressure generated by the inflow of water into the cell that is triggered by the considerable osmotic potential of the cytoplasm (7, 68). Turgor is notoriously difficult to measure, but values between 2 and 6 atm for the Gram-negative bacterium *Escherichia coli* and between 20 and 30 atm for the Gram-positive bacteria *Bacillus subtilis* and *Staphylococcus aureus*, respectively, have been reported (5, 67). Turgor is resisted by the peptidoglycan sacculus, a microbial exoskeleton that provides mechanical stability and shape to the cell (26, 61, 63). Although the peptidoglycan sacculus is a firm supermacromolecular structure, it is also highly dynamic, since the cell has to continuously weave new building blocks into the existing mesh of the peptidoglycan as it elongates and finally divides (22, 63, 66). To allow the extension and remodeling of the existing peptidoglycan sacculus, autolysins cleave bonds both in the sugar backbone and in the interconnecting peptide bridges (55, 62, 63).

The tension (30) that is applied onto the peptidoglycan sacculus is influenced by fluctuations in the external osmolarity (7, 68). Turgor increases due to water influx when the cell is exposed to hypoosmotic environments, and it decreases when the cell is confronted by hyperosmotic circumstances in response to water efflux (7, 32, 69). Microorganisms actively adjust their turgor to the prevailing external osmolarity by dynamically modulating the osmotic potential of their cytoplasm through the accumulation (at high osmolarity) and expulsion (at low osmolarity) of water-attracting ions and organic solutes (5, 32, 69). Although active water management is certainly the cornerstone of the microbial stress response to osmotic changes, the overall cellular process of acclimatization to fluctuations in environmental osmolarity is quite complex. This has been exemplified through detailed studies with the soil bacterium *Bacillus subtilis* (20, 27, 28, 58), whose primary habitat, the upper layers of the soil, is frequently subjected to both decreases and increases in osmolarity caused by flooding and desiccation (6).

Genome-wide transcriptional profiling studies of *B. subtilis* cells cultivated under sustained high-salinity conditions (58) revealed upregulation in the transcription not only of genes involved in the uptake and production of osmoprotectants (6, 7) but also of a number of genes involved in peptidoglycan synthesis and the remodeling of the peptidoglycan sacculus. Among the approximately 100 osmotically upregulated genes identified previously by Steil et al. (58) is *gpsB* (*ypsB*), a gene encoding a key player in the elongation-division cycle of the *B. subtilis* cell that recruits penicillin-binding protein 1 (PBP1) to the cell division site (10). The osmotic induction of the structural gene (*pbpE*) for the peptidoglycan endopeptidase PBP4* has also been observed (47), and the individual disruption of the *gpsB* and *pbpE* genes causes osmotic sensitivity (10, 47). Among the osmotically regulated genes of *B. subtilis* (58) are also *yocH*, which encodes a cell wall-associated muralytic enzyme that cleaves the sugar backbone of murein (53); the structural gene for the YocH-related YabE protein, whose peptidoglycan hydrolytic activity might allow a renewed cell wall growth of dormant *B. subtilis* cells (14); and *yqiI*, which is predicted to encode a secreted *N*-acetylmuramoyl-L-alanine amidase (55). Finally, the expression of the gene encoding the muro-

TABLE 1 *B. subtilis* strains used in this study

Strain[a]	Relevant genotype	Source or reference
168	*trpC2*	Laboratory collection
JGB34	Δ(*treA::ery*)2	J. Gade
TSTB3	Δ(*treA::neo*)1	57
rok	Δ(*rok::neo*)	1
KFB8	Δ(*yqiHIK::neo*)1	This study
KFB9	Δ(*lytC::spc*)1	This study
KFB10	Δ(*yrvJ::ery*)1	This study
KFB16	Δ(*cwlC::tet*)1	This study
KFB17	Δ(*cwlD::ble*)1	This study
KFB37	Δ(*yqiHIK::neo*)1 Δ(*lytC::spc*)1 Δ(*yrvJ::ery*)1 Δ(*cwlC::tet*)1 Δ(*cwlD::ble*)1	This study
KFB15	*amyE*::[φ(*yqiH*$_{300\,bp}$′-*treA*) *cat*] Δ(*treA::neo*)1	This study
KFB41	*amyE*::[φ(*yqiH*$_{300\,bp}$′-*treA*) *cat*] Δ(*treA::ery*)2	This study
KFB47	*amyE*::[φ(*yqiH*$_{300\,bp}$′-*treA*) *cat*] Δ(*treA::ery*)2 Δ(*rok::neo*)	This study

[a] All strains are derivatives of *B. subtilis* wild-type strain 168 (3) and therefore also carry the *trpC2* mutation. The genetic designation *amyE*::[φ(*yqiH*′-*treA*) *cat*] indicates that the reporter fusion is integrated as a single copy into the genome at the *amyE* locus via a double-recombination event; the *amyE* gene is consequently disrupted, and all fusions strains therefore possess an AmyE⁻ phenotype.

peptidase LytF, a major autolysin of *B. subtilis* (42), is strongly repressed under high-salinity growth conditions (58).

Taken together, these data leave the impression that changes in the murein sacculus take place when the *B. subtilis* cell is continuously confronted with hyperosmotic growth conditions. This notion is reinforced by data reported previously by Lopez et al. (39, 40), who observed variations in the envelope composition of osmotically stressed *B. subtilis* cells, leading to altered susceptibilities to antibiotics targeting the cell wall and to several bacteriophages. Although the cell wall of *B. subtilis* apparently increases in thickness under high-salinity growth conditions (47), the underlying architectural changes are far from clear.

To begin a more detailed analysis of this process and to foster an understanding of the regulation of those osmotically regulated genes encoding peptidoglycan-hydrolyzing and -modifying enzymes, we focus here on the predicted *N*-acetylmuramoyl-L-alanine amidase YqiI. We found that the *yqiI* gene is embedded in the *yqiHIK* operon and discovered that an enhanced expression of the *yqiHIK* promoter is triggered only under growth conditions that constitute a considerable degree of osmotic stress for the *B. subtilis* cell. Mapping and mutational analysis of the *yqiHIK* promoter and its flanking regions uncovered key determinants for its osmotic control and revealed an AT-rich DNA segment located 180 bp upstream of the −35 region upon which the osmotic induction and activity of the *yqiHIK* promoter were strictly dependent.

MATERIALS AND METHODS

Chemicals. The chromogenic substrate for the TreA enzyme, *para*-nitrophenyl-α-D-glucopyranoside (α-PNPG); anhydrotetracycline (AHT); as well as the antibiotics ampicillin, chloramphenicol, erythromycin, kanamycin, and spectinomycin were purchased from Sigma-Aldrich (Steinheim, Germany). The antibiotic zeocin was purchased from Invitrogen (Carlsbad, CA).

Bacterial strains. *E. coli* strain DH5α (Invitrogen, Carlsbad, CA) was used for all routine cloning experiments. For the overproduction of the recombinant YqiI–Strep-tag-II protein, we employed *E. coli* B strain BL21(arctic express[DE 3]RIL) (Stratagene, La Jolla, CA). All *B. subtilis* strains used in this study were derived from strain 168 (3), a domesticated line of *B. subtilis* laboratory strains; these strains are listed in Table 1.

Media and growth conditions. *E. coli* and *B. subtilis* were propagated and maintained on Luria-Bertani (LB) agar plates. The various *B. subtilis* strains were cultivated in Spizizen's minimal medium (SMM). This chemically defined medium contained 0.5% (wt/vol) glucose as the carbon source, a solution of trace elements (21), and L-tryptophan (20 mg liter⁻¹) to satisfy the auxotrophic needs of *B. subtilis* strain 168 and its derivatives (Table 1). The growth of bacterial cultures was monitored spectrophotometrically at a wavelength of 578 nm (optical density at 578 nm [OD$_{578}$]). *B. subtilis* cultures were routinely grown aerobically at 37°C in 100-ml Erlenmeyer flasks with a culture volume of 20 ml in a shaking water bath set at 220 rpm. All cultures were inoculated from exponentially growing precultures (grown in SMM) to an OD$_{578}$ of 0.1. For osmotic stress experiments, the salinity of the medium was increased by the addition of NaCl from a concentrated stock solution (5 M) prepared in distilled water. The production of the extracellular α-amylase AmyE by *B. subtilis* strains was analyzed by the starch iodine test (11). The antibiotics chloramphenicol (5 µg ml⁻¹), erythromycin (1 µg ml⁻¹), kanamycin (10 µg ml⁻¹), zeocin (35 µg ml⁻¹), tetracycline (15 µg ml⁻¹), and spectinomycin (100 µg ml⁻¹) were used for the selection of *B. subtilis* strains carrying an antibiotic resistance cassette integrated into the genome. For *E. coli* cultures carrying a plasmid, ampicillin was used at a final concentration of 100 µg ml⁻¹.

Genetic construction of *B. subtilis* mutant strains. To construct a deletion of the *yqiHIK* gene cluster, the flanking 5′ and 3′ regions were amplified by PCR from chromosomal DNA of *B. subtilis* wild-type strain 168 and connected by long-flanking-region PCR (35) with the gene for a kanamycin resistance cassette derived from plasmid pDG783 (19). *B. subtilis* strain 168 was then transformed with the resulting PCR product, which yielded strain KFB8 [Δ(*yqiHIK::neo*)1] (Table 1). In a similar way, gene disruption mutations in the *lytC*, *yrvJ*, *cwlC*, and *cwlD* amidase genes were constructed (Table 1), and chromosomal DNA isolated form each of these mutant strains was used to obtain *yqiHIK lytC yrvJ cwlC cwlD* quintuple mutant strain KFB37 (Table 1). The Δ*rok*::*neo* mutant allele (1) (Table 1) was moved into other *B. subtilis* genetic backgrounds by transforming the recipient strain with chromosomal DNA of the donor strain and subsequent selection for kanamycin-resistant transformants. The *yqiH-treA* operon fusion located on plasmid pKF13 is linked to a chloramphenicol resistance gene (*cat*), and the entire construct is flanked by the 5′ and 3′ segments of the *amyE* gene. To integrate the reporter gene fusion as a single copy into the *B. subtilis* genome at the *amyE* site via a double-recombination event, DNA of plasmid pKF13 was cut with XhoI, and *B. subtilis* strains TSTB3 (Δ*treA::neo*) and JGB34 (Δ*treA::ery*) (Table 1) were then transformed with the linearized DNA, thereby yielding strains KFB15 and KFB41, respectively (Table 1). The resulting strains exhibited the expected AmyE⁻ phenotype, as judged by the starch iodine test (11). Derivatives of plasmid pKF13 (*yqiH-treA*) carrying either point mutations in the *yqiH* promoter or deletions covering regions located upstream of this promoter were integrated into the *B. subtilis* genome at the *amyE* site in a similar manner.

Recombinant DNA techniques and construction of plasmids. Routine manipulations of plasmid DNA, PCR, the construction of recombinant DNA plasmids, the isolation of chromosomal DNA from *B. subtilis*, and the transformation of bacterial cells with plasmid or chromosomal DNA were carried out by using standard procedures (11, 51). To construct an overexpression system for the *B. subtilis yqiI* gene, a 555-bp DNA fragment covering the *yqiI* coding region (except for its signal sequence) was prepared by PCR using primers carrying BsaI restriction sites at their ends; the PCR product was cleaved with BsaI and inserted into plasmid pASK-IBA3 Plus (IBA, Göttingen, Germany), which had been cut with the same restriction enzyme. This generated a hybrid gene where the *yqiI* coding region was fused at its 3′ end with a short DNA sequence encoding a Strep-tag-II affinity peptide. The expression of this gene on the resulting plasmid, pKF11, was mediated by the TetR-responsive *tet* promoter carried by the vector pASK-IBA3 Plus. To facilitate the mapping of the *yqiHIK* promoter, we prepared by PCR a 546-bp DNA fragment covering the regulatory region and part of the *yqiH* coding region, cleaved it with EcoRI, and inserted this DNA fragment into the *E. coli–B. subtilis* shuttle

vector pRB373 at its unique EcoRI site (9). The resulting plasmid, pKF16, was used to transform *B. subtilis* wild-type strain 168 by selecting for kanamycin-resistant colonies. To construct reporter gene fusions to the *yqiHIK* promoter/regulatory region, we used plasmid pJMB1 (M. Jebbar and E. Bremer, unpublished data), which carries a promoterless *treA* gene encoding a highly salt-tolerant phospho-α-(1,1)-glucosidase (TreA) (17). A 300-bp DNA fragment of the *yqiHIK* promoter region (see Fig. 6A) was amplified by PCR from chromosomal DNA of wild-type strain 168, cleaved with the restriction enzymes BamHI and SmaI, and inserted into the vector pJMB1, which had been linearized with the same restriction enzymes. A deletion analysis of the *yqiHIK* regulatory region was carried out by systematically shortening the 5′ region while maintaining the junction of the *treA* and *yqiH* genes present in the parent *yqiH-treA* operon fusion (see Fig. 6A). The resulting PCR fragments, with sizes of 279 bp, 270 bp, and 250 bp, were inserted into *treA* reporter plasmid pJMB1 as described above. Mutant derivatives of the *yqiHIK* −35 and −10 promoter regions were generated with the QuikChange II XL site-directed mutagenesis kit (Stratagene, La Jolla, CA), using DNA of *yqiH-treA* fusion plasmid pKF13 as the template and custom-synthesized DNA primers. The introduction of the desired mutations into the *yqiHIK* promoter was verified by DNA sequencing (Eurofins MWG Operon, Ebersberg, Germany). The mutant *yqiH-treA* operon fusion constructs were integrated into the chromosome of *B. subtilis* 168 as a single copy at the *amyE* locus, as described above. To generate a plasmid expressing the *yqiI* gene for complementation studies, we amplified the *yqiI* coding region and its ribosome-binding site by PCR and inserted this DNA fragment into plasmid pGP382, where it is expressed from the constitutive *degQ*36 promoter (25); this construct was named pKF51.

Isolation of RNA, mapping of the transcriptional organization of *yqiHIK*, and primer extension analysis of the *yqiHIK* operon. Total RNA was isolated from exponentially growing cultures (OD$_{578}$ of 0.8 to 1.0) of *B. subtilis* strain 168 carrying plasmid pKF16 (encoding the *yqiHIK* regulatory region). This strain was cultured either in SMM or in SMM with 1.2 M NaCl. We used the High Pure RNA isolation kit from Roche (Mannheim, Germany) and followed the manufacturer's protocol to obtain total RNA from 10 ml of culture aliquots. The concentration of the isolated RNA was quantified spectrophotometrically (A_{260}); an A_{260} of 1 corresponds to approximately 40 μg RNA ml^{-1} (51). To map the 5′ end of the *yqiHIK* transcript, a primer extension analysis was carried out. Ten micrograms of total *B. subtilis* RNA and 10 pmol of a *yqiH*-specific oligonucleotide (5′-ACGTTTATCCTTCGGAACTTG-3′) labeled at its 5′ end with the fluorescence dye DY-781 (Biomers, Ulm, Germany) were hybridized to each other and used for a reverse transcriptase (RT) reaction. This reaction was performed with the Primer-Extension-System-AMV reverse transcriptase kit purchased from Promega (Madison, WI). To size the 5′ end of the produced *yqiH* cDNA, a DNA sequencing reaction was performed with plasmid pKF16 as the DNA template and the DY-781 fluorescence 5′-end-labeled DNA primer described above. The primer extension products were run on a denaturing 5% polyacrylamide DNA sequencing gel alongside the DNA sequencing reaction products and were analyzed with a Li-Cor DNA sequencer (model 4000; Eurofins MWG, Ebersberg, Germany).

TreA enzyme assays. The expressions of the various *yqiH-treA* fusions were monitored by measuring the activity of the TreA [phospho-α-(1,1)-glucosidase] reporter enzyme using the chromogenic substrate α-PNPG (17). Aliquots (1.8 ml) from exponential-phase cultures (OD$_{578}$ of about 1 to 1.5) of the *B. subtilis* fusion strains were harvested by centrifugation for 5 min in an Eppendorf microcentrifuge. The cells were resuspended in 0.5 ml Z buffer (43) adjusted to pH 7, which contained 1 mg ml^{-1} lysozyme to disrupt the *B. subtilis* cell wall. After incubation of the samples for 10 min at 37°C, cellular debris were removed by centrifugation, and 0.4 ml of the supernatant was then used for TreA activity assays (23). TreA-specific enzyme activity is expressed in units mg^{-1} of protein according to the definition used for the quantification of β-galactosidase enzyme activity (43).

Overproduction and purification of the *B. subtilis* YqiI protein. For the overproduction of the YqiI–Strep-tag-II protein, cells (1 liter) of *E. coli* B strain BL21(arctic express[DE 3]RIL) (Gm^r) harboring plasmid pKF11 were grown in minimal medium A (MMA) (43) supplemented with 1 mg liter^{-1} thiamine, 1 mM MgSO$_4$, 0.2% (wt/vol) Casamino Acids, 0.5% glucose (wt/vol) as the carbon source, and 100 μg ml^{-1} ampicillin to select for the presence of plasmid pKF11. The precise cultivation procedure for the production of the recombinant YqiI–Strep-tag-II protein followed that described previously by Pittelkow et al. (48) for the production of the *B. subtilis* choline ligand-binding protein OpuBC. The recombinant YqiI–Strep-tag-II protein was purified from cleared lysates of the producer cells by affinity chromatography on a Strep-Tactin Superflow column (IBA, Göttingen, Germany). The elution buffer was adjusted to pH 7.5. The purity of the obtained YqiI–Strep-tag-II recombinant protein was assessed by SDS-PAGE, and the protein was stored at 4°C for further use in zymography.

Preparation of *B. subtilis* cell wall material and zymograms. Cell wall sacculi of *B. subtilis* 168 were prepared as reported previously by Kawai et al. (31), with minor modifications. Cells (1 liter) of an exponentially growing culture (OD$_{578}$ of 0.5 to 1.0) (in SMM at 37°C) of *B. subtilis* strain 168 were cooled in a water bath to about 4°C. The cells were then harvested by centrifugation (for 15 min at 4°C at 2,400 × *g*), and the cells were disrupted with a Bead-Beater (Braun Biotech International) (for 2 min, set at 2,000 rpm). The resulting cell powder was resuspended in 40 ml of ice-cold 50 mM Tris-HCl (pH 7.5) buffer and added dropwise to 120 ml of a boiling SDS (5%) solution that was well stirred. The suspension of the cell wall material was boiled for 15 min with stirring and subsequently chilled to room temperature. The sedimentation of the cell wall peptidoglycan was achieved by centrifuge at 21,000 × *g* for 20 min at room temperature. To remove the SDS from the cell wall sacculus preparation, the collected material was carefully washed three times with distilled water. The final pellet was dissolved in 100 μl distilled water and frozen at −20°C until further use.

The peptidoglycan hydrolase activity of the YqiI–Strep-tag-II recombinant protein was analyzed by zymography (16). An SDS-polyacrylamide gel (15% [wt/vol]) containing 0.2% (wt/vol) purified cell wall peptidoglycan was loaded with 8 μg of the purified YqiI–Strep-tag-II protein. Following electrophoresis of the protein at 20 mA at a constant current at room temperature through the gel matrix, the SDS-polyacrylamide gel was incubated overnight in a renaturation buffer (1% Triton X-100, 20 mM MgCl$_2$, 25 mM Tris-HCl [pH 7.5]) at 37°C with gentle shaking (16). The cell wall hydrolytic activity of YqiI–Strep-tag-II was detected after staining of the polyacrylamide gel with 0.1% methylene blue (dissolved in 0.01% KOH) for 3 h and subsequent destaining in distilled water.

Light microscopy. The morphologies of wild-type *B. subtilis* strain 168 and isogenic derivatives lacking various amidases (Table 1) were visualized with an Eclipse 50i (Nikon) microscope equipped with a Nikon DS-5Mc camera. Prior to microscopy, the cells were immobilized on a 1% (wt/vol) agarose pad prepared on a microscope slide. Images of the *B. subtilis* cells were recorded with the DS-5Mc camera and prepared for presentation with NIS Elements F 2.30 (Nikon) and Adobe Photoshop Elements (version 10).

Fluorescence microscopy. We assed the viability of *B. subtilis* cells by a two-color fluorescence assay, using the Live/Dead bacterial viability kit (Molecular Probes-Invitrogen, Carlsbad, CA) according to the instructions of the manufacturer. The mixture of the Syto 9 and propidium iodine stains detects bacteria with intact cytoplasmic membranes as fluorescent green cells, whereas bacteria with damaged membranes stain fluorescent red. The cells were observed with an Eclipse 50i (Nikon) microscope fitted with an appropriate filter set that allowed the detection of the red and green fluorescent stains. The excitation/emission maxima for these dyes are about 480/500 nm, respectively, for the Syto 9 stain and 490/635 nm, respectively, for propidium iodine. Pictures of the fluorescent cells were taken with a Nikon DS-5Mc camera.

Scanning electron microscopy. *B. subtilis* cells were cultured in SMM or in SMM containing 1.2 M NaCl until they reached the early exponential phase (OD_{578} of 0.7 to 0.9). The cells were then immobilized on a nylon membrane (Pall BioSupport, East Hills, NY) and subsequently fixed with 1% (vol/vol) glutaraldehyde. Cells attached to the nylon membrane were washed with Sörensen buffer (100 ml KH_2PO_4 of a 0.1 M stock solution, 900 ml $NaHPO_4$ of a 0.1 M stock solution [pH 7.8]) and postfixed (for 2 h) with 1% (vol/vol) osmium tetraoxide. After the fixed cells were washed three times with Sörensen buffer and distilled water, the cells were dehydrated overnight in ethylene glycol ethyl ether and then stored in 100% (vol/vol) acetone. The dehydrated samples were then dried by a critical-point drier under a CO_2 atmosphere and were subsequently coated with gold. The cells were visualized with the aid of a Hitachi S-530 scanning electron microscope.

Database searches, amino acid sequence alignments, and modeling of the YqiI structure. Proteins homologous to the YqiI protein from *B. subtilis* were identified via the GenoList Web server (http://genodb.pasteur.fr/cgi-bin/WebObjects/GenoList). The domain structures of these proteins were analyzed by using the SMART (Simple Modular Architecture Research Tool) Web tool (http://smart.embl-heidelberg.de/) (38). The identified protein domains are named according to the Pfam nomenclature scheme (49). The alignment of the amino acid sequences of proteins related to YqiI was performed with ClustalW (59). An *in silico* model of the *B. subtilis* YqiI protein was obtained with the aid of the SWISS Model server (http://swissmodel.expasy.org/) (2), using the crystallographic data set deposited under PDB accession number 1JWQ for the CwlV protein from *Paenibacillus polymyxa* var. *colistinus* as the modeling template. The figure of the YqiI *in silico* model was prepared with PyMOL (http://www.pymol.org/).

RESULTS

The *yqiHIK* gene cluster is transcribed as an operon. The *yqiI* gene is flanked by the *yqiH* and *yqiK* genes (Fig. 1A), and they are predicted to encode an extracellular lipoprotein (YqiH), a secreted amidase (YqiI), and a cytoplasmic glycerophosphodiester phosphodiesterase (YqiK). In the genome-wide transcriptional profiling analysis of salt-stressed *B. subtilis* cells reported previously by Steil et al. (58), the expressions of both the *yqiH* and *yqiI* genes were strongly upregulated in response to osmotic stress (15-fold and 7-fold, respectively); however, the degree of osmotic induction of the *yqiK* gene did not pass the imposed threshold level (3-fold), but an osmotic induction of *yqiK* expression was recorded. This data set therefore suggests that the *B. subtilis yqiHIK* genes might be transcribed as an osmotically inducible operon.

To test the possible cotranscription of the *yqiHIK* genes, we isolated total RNA from cells of *B. subtilis* wild-type strain 168 and performed one-step reverse transcriptase PCR with primers that covered the intergenic regions of the *yqiHIK* gene cluster. The data documented in Fig. 1B demonstrate that the *yqiHIK* genes are indeed cotranscribed. In all likelihood, the *yqiHIK* transcript ends at an intrinsic terminator sequence found in the 137-bp intragenic region between the *yqiK* gene and the downstream *mmgA* gene (transcribed in the same direction as *yqiHIK*), which encodes a degradative acetoacetyl coenzyme A (CoA) thiolase (50). Indeed, this conclusion is fully consistent with data from a recently reported comprehensive tiling-array study by Nicolas et al. (46). Those authors also presented evidence for the presence of an internal promoter positioned in front of *yqiK*. A gene neighborhood analysis (http://img.jgi.doe.gov/) revealed the existence of *yqiHIK* gene clusters only in three close relatives of *B. subtilis*: *Bacillus amyloliquefaciens*, *Bacillus atropheus*, and *Bacillus licheniformis*.
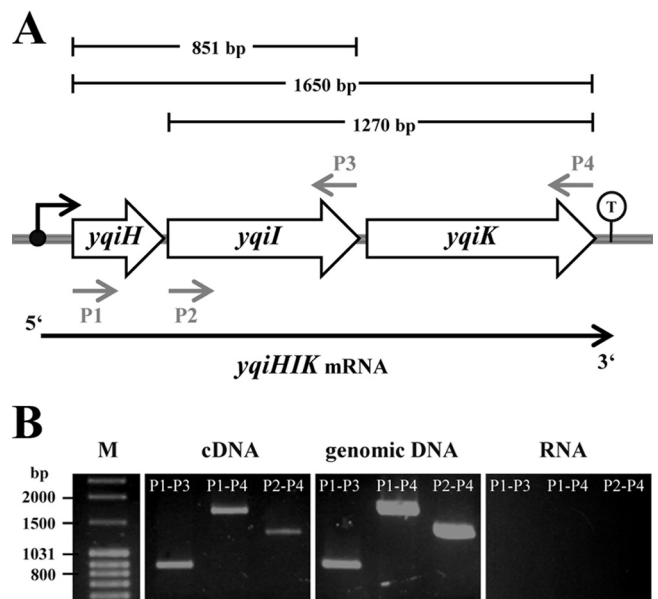

FIG 1 Structure and genetic organization of the *yqiHIK* gene cluster. (A) Genetic map of the *yqiHIK* genes in the genome of *B. subtilis*. The length and the position of the different PCR-amplified fragments are indicated. A bent arrow indicates the promoter region and the direction of *yqiHIK* transcription; the position of a putative factor-independent transcriptional terminator sequence is marked by a lollipop. (B) RT-PCR-based analysis of the putative *yqiHIK* operon. The amplification reactions using the indicated DNA primers (P1 to P4) were conducted on different templates: cDNA, genomic DNA as a positive control, and RNA as a negative control. Total RNA was isolated from cells of *B. subtilis* strain 168 grown in SMM. M, molecular marker.

The YqiI protein possesses cell wall hydrolytic activity. To study the functional role of the *yqiHIK* gene cluster further, we focused our analysis on the biochemical properties of the YqiI protein, which is predicted to serve as an *N*-acetylmuramoyl-L-alanine amidase (55). It therefore should possess cell wall hydrolytic activity. To test this prediction, we produced a recombinant YqiI–Strep-tag-II protein in *E. coli*, purified it by affinity chromatography (Fig. 2, left), and used zymography (16, 29) to assess its cell wall hydrolytic activity toward peptidoglycan isolated from *B. subtilis* strain 168. Figure 2, right, shows that the YqiI–Strep-tag-II protein can indeed hydrolyze peptidoglycan, and this observed enzymatic activity is therefore consistent with the predicted *in silico* function (55) of YqiI as an *N*-acetylmuramoyl-L-alanine amidase.

In silico assessment of the amidase_3 domain of YqiI and four of its homologues in *B. subtilis*. The analysis of the sequence of the 206 amino acids comprising the YqiI protein via the SMART Web tool (38) revealed the presence of a signal sequence (amino acids 1 to 23) for the Sec-mediated export of YqiI across the cytoplasmic membrane and an amidase_3 domain (from amino acids 67 to 178 of the mature protein), a domain which is found in many *N*-acetylmuramoyl-L-alanine amidases (15, 55, 62). This domain is present in the crystal structure of the catalytically active domain (CwlV1) of the cell wall hydrolase CwlV from *Paenibacillus polymyxa* var. *colistinus* (PDB accession number 1JWQ). We used the crystallographic data set reported for the CwlV protein and the Web-based SWISS Model server (2) to derive an *in silico* model of the *B. subtilis* YqiI amidase (Fig. 3C). The
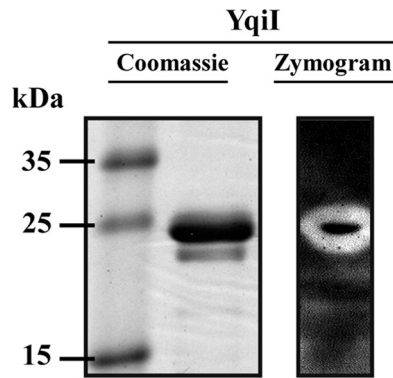
FIG 2 Cell wall hydrolase activity of the purified YqiI–Strep-tag-II protein. (Left) Coomassie blue-stained SDS-PAGE gel of the affinity purified YqiI–Strep-tag-II protein. (Right) Zymogram analysis (16) using purified *B. subtilis* 168 sacculi. Staining of the polyacrylamide gel with methylene blue and destaining with distilled water detected areas of peptidoglycan lysis. Eight micrograms of the purified YqiI–Strep-tag-II protein was applied for both SDS-PAGE and the zymogram.

predicted YqiI structure consists of a mixed β-sheet and five α-helices. This *in silico* model allowed the visualization of the positions of those residues (H-15, E-29, and H-82) that are known to be involved in coordinating the catalytically important zinc ion in *N*-acetylmuramoyl-L-alanine amidases (15), including that present in the CwlV enzyme (54), upon which the crystal structure of our YqiI *in silico* model is based. Our YqiI *in silico* model also highlights the position of residue E-148 (Fig. 3C), a residue that is critical for the biochemical functioning of *N*-acetylmuramoyl-L-alanine amidases (15, 54). We note that apparently no cell wall-binding domain is present in the YqiI protein (Fig. 3B), as suggested by an analysis of the YqiI amino acid sequence with the SMART Web tool (38).

Four additional proteins (LytC, CwlC, CwlD, and YrvJ) that exhibit a modest level of amino acid sequence identity to YqiI, ranging between 12 and 32%, are present in *B. subtilis*. Like YqiI, each of these proteins possesses an amidase_3 domain in which the above-discussed residues for the biochemical functioning of amidases are strictly conserved (Fig. 3A). The amino acid sequence identities of the catalytic domains found in the YqiI, LytC, CwlC, CwlD, and YrvJ proteins range between 33 and 55% (Fig. 3A). Three of the four proteins related to YqiI have already been functionally studied. LytC is the major autolysin of vegetative *B. subtilis* cells (34, 37, 70), whereas CwlC and CwlD play important roles during spore formation and germination (44, 52). No functional data are yet available for the YrvJ protein. LytC, CwlC, and YrvJ possess potential cell wall-retaining domains that belong to different subgroups (49): PF04122 for LytC, PF05036 for CwlC, and SM00287 for YrvJ (Fig. 3B). CwlD lacks such readily recognizable cell wall-retaining domains (Fig. 3B), but charged amino acids at the N terminus followed by a hydrophobic region have been implicated in the binding of CwlD to the spore membrane (52). Such a motif is not present in YqiI.

Deletion of the *yqiHIK* operon impairs growth of *B. subtilis* at high salinity. In view of the fact that the transcription of the *yqiHIK* gene cluster is induced under hyperosmotic conditions (58), we assessed the growth properties of Δ(*yqiHIK*::*neo*)*1* mutant strain KFB8 both in SMM and in SMM containing 1.2 M NaCl. Its growth in SMM was impaired in comparison to that of its parent strain, 168 (25), and this was also observed when this strain was cultured in high-osmolarity minimal medium. However, the culture of strain KFB8 [Δ(*yqiHIK*::*neo*)*1*] eventually reached the same optical density as that of the culture of the wild-type strain (Fig. 4B). The osmotic sensitivity of the *yqiHIK*::*neo* deletion strain could be rescued by expressing the *yqiI* gene on a pGP382-derived (25) plasmid (pKF51) under the control of the constitutive *degQ36* promoter (see Fig. S1 in the supplemental material).

We constructed a set of strains carrying gene disruption mutations for the YqiI-related LytC, CwlC, CwlD, and YrvJ proteins (Table 1) and tested their growth properties in high-salinity minimal medium. Each of these strains grew similarly to Δ(*yqiHIK*::*neo*)*1* mutant strain KFB8 in both SMM and SMM with 1.2 M NaCl (data not shown). We then combined the individual mutations in these genes with that in *yqiI*; the growth properties of quintuple mutant strain KFB37 (*lytC cwlC cwlD yrvJ yqiI*) revealed no significant differences from the growth properties of strain KFB8 either in SMM or in SMM with 1.2 M NaCl (Fig. 4A and B). Consequently, a *B. subtilis* mutant strain lacking all *N*-acetylmuramoyl-L-alanine amidases and possessing an amidase_3 domain (Fig. 3B) is viable under both growth conditions. It is known that mutations in certain amidases of *B. subtilis* impair cell motility (LytC) or the germination of spores (CwlD) (37, 52). We therefore tested whether the loss of the *yqiHIK* operon would also cause such phenotypes, but we detected no effects on cell motility and the formation of vegetative cells from heat-resistant endospores (see Fig. S2 and S3 in the supplemental material).

Morphological deformations and their reversal to a rod-shaped morphology during acclimatization of *B. subtilis* to high-salinity surroundings. While studying the growth properties of the *yqiHIK* mutant and its parent strain, 168, at high salinity (Fig. 4B), we monitored cell morphology by phase-contrast microscopy. We observed remarkable changes in cell morphology as the cells adjusted their growth to the high-salinity medium. In these experiments, the *B. subtilis* cells were precultured (to an OD_{578} of about 1 to 1.5) in SMM and were then used to freshly inoculate (to an OD_{578} of about 0.1) high-salinity medium (SMM with 1.2 M NaCl). This shift from a moderate-osmolarity (340 mosmol kg of water^{-1}) to a high-osmolarity (2700 mosmol kg of water^{-1}) environment constitutes a harsh osmotic upshock (4), to which the *B. subtilis* cells react with a considerable lengthening of the lag phase (Fig. 4B) in comparison to that observed for cells inoculated into SMM (Fig. 4A). The cells of wild-type strain 168 initially exhibited the rod-shaped morphology typical of *B. subtilis* cells (Fig. 4C). As the cells began to adjust to the new high-salinity conditions and slowly started to grow, they underwent gross morphological changes that were manifested as a curving of the cells and bulging at their ends (Fig. 4C). Such morphological deformations were no longer detectable when the cells had completely adjusted to the high-salinity environment and had entered the exponential growth phase (Fig. 4C). The scanning electron micrographs of wild-type strain 168 cells shown in Fig. 5B and C highlight these morphological aberrations. They point to a considerable degree of heterogeneity in cell morphology during the period of acclimatization of *B. subtilis* cells to a high-salinity environment.

yqiI mutant strain KFB8 and the strain carrying the simultaneous disruption of the *lytC*, *cwlC*, *cwlD*, *yrvJ*, and *yqiI* genes (KFB37) also exhibited such morphological changes (Fig. 4C).
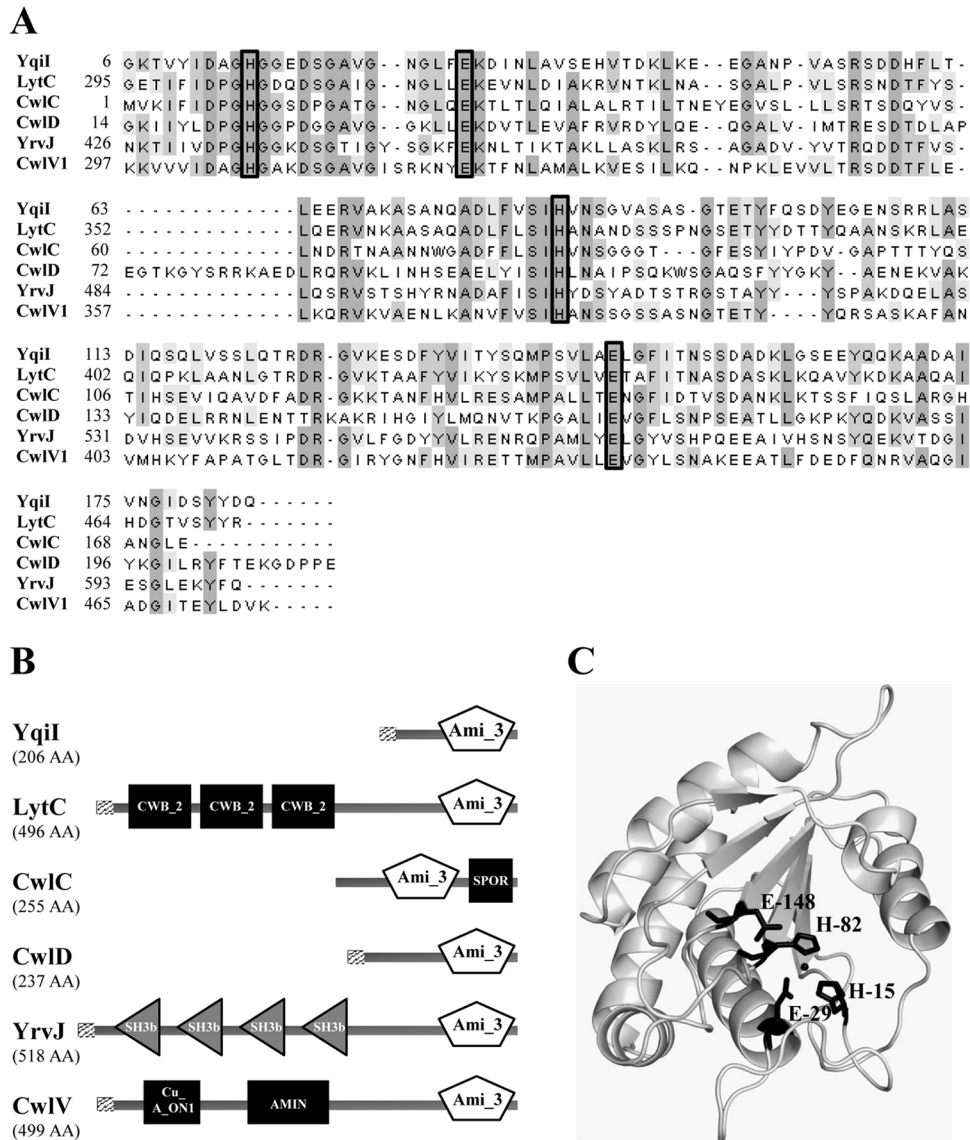
A

B

C

FIG 3 *In silico* analysis of the YqiI protein. (A) Alignment of the amino acid (AA) sequences (catalytic domain only) of the YqiI, LytC, CwlC, CwlD, and YrvJ proteins from *B. subtilis* and the CwlV1 protein from *P. polymyxa* var. *colistinus*. Black boxes highlight amino acids that are involved in the coordination of a zinc ion in the active site of amidases (15, 54). (B) Domain organization of *B. subtilis* proteins homologous to YqiI. The lengths of the proteins are indicated. Boxes with hatch marks represent Sec-type signal sequences; they are present in all amidases shown except for CwlC. The amidase_3 (Ami_3) domain (PF015020) is marked. Black boxes and gray triangles represent different types of cell wall-binding domains: cell wall-binding domain 2 (CWB_2) (PF04122) of LytC, the spore domain (SPOR) of CwlC (PF05036), the SH3b domain of YrvJ (SM00287), and the amine domain (AMIN) (PF11741) of CwlV. (C) *In silico* model of YqiI based on the crystal structure of the catalytic domain of the CwlV1 protein (PDB accession number 1JWQ) from *P. polymyxa* var. *colistinus*. The amino acids H-15, E-29, H-82, and E-148 are predicted to coordinate a zinc ion in the active center of the protein and contribute to enzyme activity.

Both the wild type and the *yqiI* and *lytC cwlC cwlD yrvJ yqiI* quintuple mutant strains regained the typical rod-shaped morphology of *B. subtilis* cells when the cells had fully acclimatized to the high-salinity growth conditions and grew exponentially (Fig. 4B and C). These microscopic observations therefore suggest that the LytC, CwlC, CwlD, YrvJ, and YqiI amidases are not critically involved in the reshaping of the rod-shaped morphology of *B. subtilis* cells as they transit from low-osmolarity to high-osmolarity surroundings. We assessed the viability of the morphologically distorted cells of both wild-type strain 168 and its mutant derivatives KFB8 and KFB37 with the "live-dead" staining procedure and found that a large fraction of the deformed cells were alive (Fig. 5A).

Osmotic regulation of the *yqiHIK* gene cluster. To provide a quantitative analysis of the osmotically induced regulation of the *yqiHIK* gene cluster (58), we constructed a *yqiH-treA* reporter gene fusion. For this purpose, a 300-bp DNA fragment carrying the beginning of the *yqiH* coding region and 257 bp of upstream sequences (Fig. 6A) was fused to the promoterless *treA* reporter gene (17). This transcriptional fusion construct was stably integrated as a single copy into the *B. subtilis* chromosome through a double-homologous-recombination event, thereby yielding strain KFB15. We grew strain KFB15 in SMM containing various concentrations of NaCl and then determined the TreA activity of cells grown to the early (OD_{578} of about 1 to 1.5) exponential
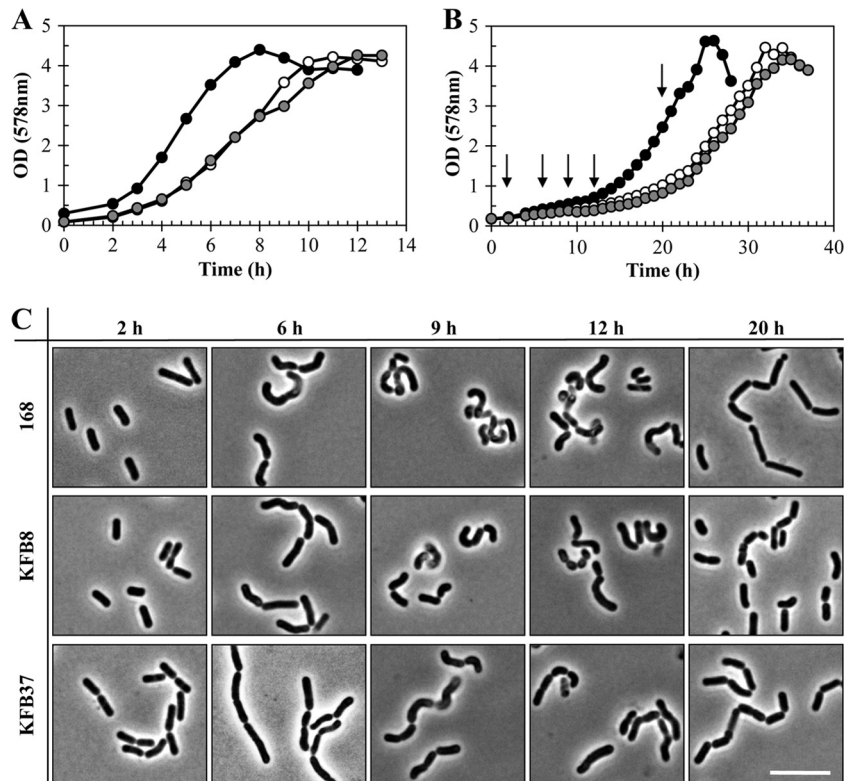
FIG 4 Growth properties of *yqiHIK* deletion mutant strain KFB8 and strain KFB37 (*lytC cwlC cwlD yrvJ yqiI*). (A and B) Cultures of *B. subtilis* wild-type strain 168 (black circles), its Δ(*yqiHIK*::*neo*) derivative strain KFB8 (white circles), and the *lytC cwlC cwlD yrvJ yqiI* quintuple mutant strain KFB37 (gray circles) were grown in SMM alone (A) or in SMM containing 1.2 M NaCl (B). (C) The morphologies of *B. subtilis* strains 168, KFB8, and KFB37 were analyzed by phase-contrast microscopy at different time points (indicated by arrows) during the growth of the cultures. Scale bar, 5 μm.

phase. Strikingly, the expression of the *yqiH-treA* reporter fusion remained at a low basal level until the salinity of the growth medium exceeded 0.7 M NaCl. Subsequent increases in the NaCl content of the growth medium then led to a finely tuned increase in the expression level of the *yqiH-treA* reporter fusion (Fig. 7A). Hence, the *yqiHIK* gene cluster is expressed at a significant level only in *B. subtilis* strains that experience a considerable level of osmotic stress (at least 1,670 mosmol kg of water^{-1}) (Fig. 7A).

We mapped the promoter that drives *yqiHIK* gene expression under hyperosmotic conditions by primer extension analysis (Fig. 7B). The observed 5′ end of the osmotically induced transcript is positioned 25 nucleotides in front of the GTG start codon of the *yqiH* reading frame (Fig. 7B and C). An inspection of the DNA sequence upstream of the mRNA start site revealed regions that correspond to −10 and −35 sequences of SigA-type promoters of *B. subtilis* (24) and that these conserved regions are separated by 17 bp (Fig. 7C), the most preferred spacing of SigA-responsive promoters (24).

Site-directed mutagenesis of the osmoregulated *yqiHIK* promoter. To further study the characteristics of the osmotically controlled *yqiHIK* promoter, we carried out a site-directed mutagenesis experiment on key elements of this promoter. DNA sequence inspection suggested that the *yqiHIK* promoter is a SigA-type promoter, a type of *B. subtilis* promoter that is strongly dependent on a highly conserved T/A base pair in the −10 region, the so-called invariant T, for its functioning (24). Indeed, when we changed this T/A base pair to a G/C base pair in the *yqiHIK* promoter, promoter activity was lost (Table 2).

Several deviations from the canonical −10 and −35 regions of SigA-type promoters (24) are present in the *yqiHIK* promoter (Table 2). We changed the actual *yqiHIK* −35 and −10 regions stepwise to that of the DNA sequence of a consensus SigA-type promoter. The −35 region of the *yqiHIK* promoter deviates from the consensus sequence at just one position. The creation of a perfect −35 region (strain KFB24) had no significant influence on osmotic induction but slightly improved the activity of this promoter variant under hyperosmotic conditions (Table 2). The −10 region of the *yqiHIK* promoter is A/T rich but differs at three positions from that of the consensus sequence (Table 2). An improvement of the −10 region by a point mutation (strain KFB26) retained the osmotic induction of the promoter activity but allowed a somewhat higher level of expression under osmotic stress conditions (Table 2). However, the creation of a perfect fit to the consensus −10 sequence (strain KFB32) yielded a very different pattern of promoter activity, since the expression of the *yqiH-treA* reporter fusion became constitutive and exhibited a high level of activity. Similarly, a *yqiHIK* promoter variant (strain KFB34) with a combined perfect fit to SigA-type −10 and −35 sequences also resulted in a constitutive promoter (Table 2). This synthetically generated SigA-type promoter was 60-fold more active under low-osmolarity growth conditions and about 8.7-fold more active under high-osmolarity conditions than the natural *yqiHIK* promoter (Table 2).

Many *B. subtilis* SigA-type promoters carry a conserved TG motif in the −16 region, and this TG motif often contributes significantly to promoter strength and functioning (24, 65). In-
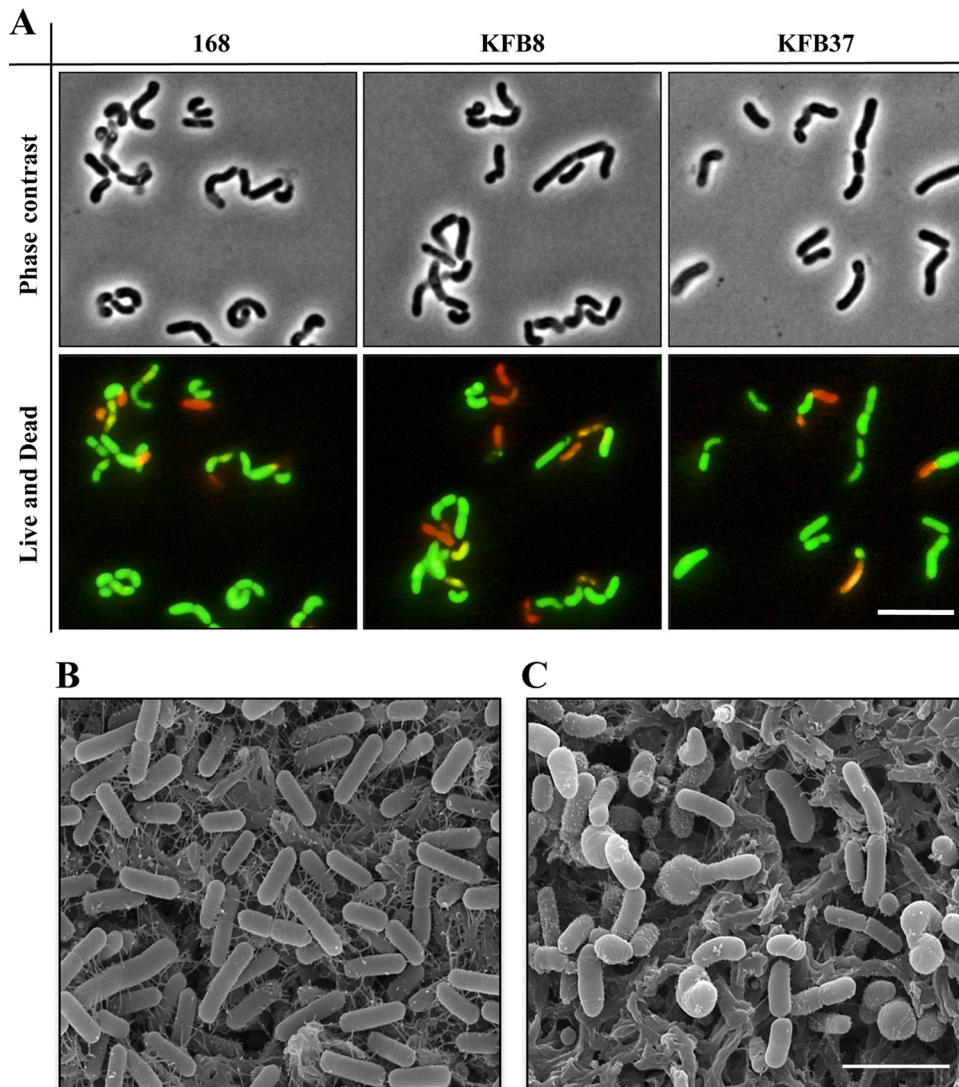
FIG 5 Fluorescence and scanning electron microscopy of salt-stressed *B. subtilis* cells. (A) Cells of wild-type strain 168 and its mutant derivatives KFB8 (*yqiHIK*) and KFB37 (*lytC cwlC cwlD yrvJ yqiI*) were grown in SMM with 1.2 M NaCl for 12 h (time point 4) (Fig. 4B) and observed by both phase-contrast and fluorescence (after staining with the Live/Dead BacLight bacterial viability kit) microscopy. Scale bar, 5 μm. (B and C) Cultures of strain 168 were grown to the early exponential phase (OD$_{578}$ of 0.7 to 0.9) in SMM alone (B) or in SMM containing 1.2 M NaCl (C) and were observed by scanning electron microscopy. The magnification was set at ×8,000, and the scale bar represents 4 μm.

stead of a TG motif, the *yqiHIK* promoter possesses a GT sequence in its −16 region (Fig. 7C). We changed the GT sequence to the TG motif and observed that the osmotic control of the *yqiHIK* promoter (strain KFB25) was fully preserved, with an induction factor similar to that exhibited by the wild-type promoter (Table 2). However, in this promoter variant, the basal level of transcriptional activity at low salinity increased modestly (4-fold), while the level of transcriptional activity under osmotic stress conditions rose 6-fold (Table 2). As expected, the combination of the TG promoter variant with perfect −10 and −35 sequences resulted in a complete loss of osmotic induction, but we observed that it did not improve the promoter activity of the promoter with SigA-type consensus −10 and −35 regions (Table 2).

Impact of an AT-rich region located upstream of the *yqiHIK* promoter on transcription. During the visual inspection of the *yqiHIK* promoter region, we noticed a 53-bp highly AT-rich re-

gion (Fig. 6A). Since such stretches of DNA could be potential targets for regulatory proteins (41, 56) or alter the DNA structure with distant effects of promoter activity through local changes in DNA topology (12, 13), we wondered whether the 53-bp highly AT-rich region would impinge on the activity or osmotic control of the *yqiHIK* promoter. To assess a possible function of the AT-rich region, we constructed a set of deletions with endpoints located either at the borderline of the AT-rich region (Δ1) or at two positions within the AT-rich region (Δ2 and Δ3) (Fig. 6A). The Δ1 fusion construct still allowed the osmotic induction of the reporter gene fusion, but the level of promoter activity fell under both high- and low-osmolarity assay conditions about 3.5-fold (Fig. 6B). In contrast, the deletion constructs with endpoints within the AT-rich region, Δ2 and Δ3, lost osmotic control altogether and exhibited only a basal level of promoter activity (Fig. 6B). Hence, the activity of the *yqiHIK* promoter under high-os-
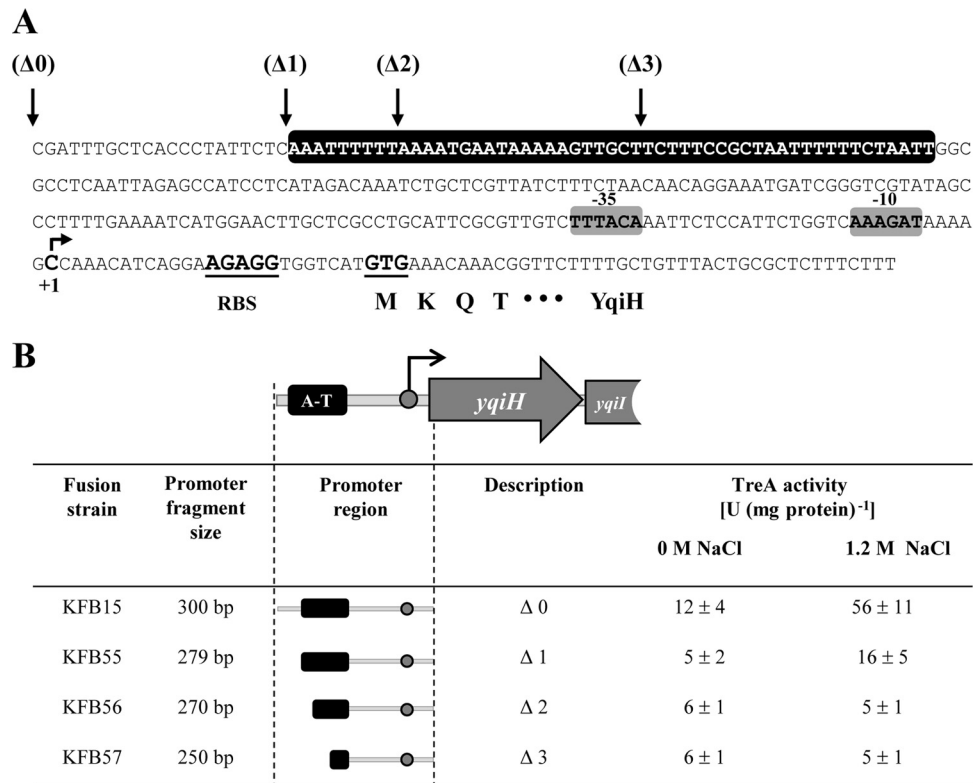
FIG 6 Influence of the AT-rich region located upstream of the *yqiHIK* promoter region on osmotic induction of *yqiH-treA* reporter gene expression. (A) DNA sequence of the 300-bp fragment fused to the promoterless *treA* reporter gene in strain KFB15. The AT-rich region is highlighted by a black box. The DNA fragment shown is defined as Δ0. Arrows indicate three different truncations (Δ1 to Δ3) of the 300-bp region originally used to construct the *yqiH-treA* gene fusion. The positions of the −35 and −10 *yqiHIK* promoter regions, the transcriptional initiation site, the ribosome-binding site of the *yqiH* gene, and its translational start codon of the *yqiH* reading frame are indicated. (B) Promoter activity and osmoregulation of reporter strains carrying the various deletion constructs in cells cultivated either in SMM or in SMM containing 1.2 M NaCl.

molarity conditions is critically dependent on an AT-rich DNA segment located a considerable distance upstream of the −35 sequence ([Fig. 6A]).

A recent study by Smits and Grossman ([56]) suggested that the Rok regulatory protein binds to many AT-rich regions in the *B. subtilis* genome. It might thus perform a function similar to that of the nucleoid-associated DNA-binding protein H-NS from *E. coli* ([12]), which participates in the control of osmotically regulated genes (e.g., the *proU* operon) ([41], [45]). We therefore wondered whether Rok might influence *yqiHIK* transcription through interactions with the AT-rich region located upstream of the −35 region ([Fig. 6A]). However, this was not the case (see Table S1 in the supplemental material).

DISCUSSION

The bacterial cell has to strike a fine balance between extending the peptidoglycan sacculus through biosynthetic activities and at the same time restraining turgor and maintaining mechanical stability. Key to these processes is a situation-conform control of those hydrolytic enzymes, the autolysins, which hydrolyze various types of chemical bonds in the peptidoglycan superstructure ([55], [62]) and therefore possess a potential cell-disruptive capability. Approximately 35 autolysins have been identified in *B. subtilis* and contribute to cell morphogenesis, motility, spore formation, and germination ([15], [55], [62]).

Here, we have focused on the YqiI protein, an *N*-acetylmuramoyl-L-alanine amidase that is predicted to cleave the amide bond between *N*-acetylmuramic acid and the first amino acid (L-Ala) of the stem peptide ([15], [55], [62]). Consistent with this prediction, the cell wall hydrolytic activity of the YqiI enzyme has been biochemically proven in this study ([Fig. 2]). YqiI possesses a Sec-type signal sequence, and it lacks readily identifiable cell wall-retaining domains ([Fig. 3B]); however, it has previously not been detected in the *B. subtilis* secretome ([60]). A cell wall-anchoring function for YqiI could potentially be provided by a coexpressed lipoprotein (YqiH) ([Fig. 1]), a possibility which has already been discussed in the context of several other autolysins ([29]).

The *yqiI* gene is embedded in an operon (*yqiHIK*) ([Fig. 1]) whose transcription is upregulated in response to severe osmotic stress ([Fig. 7A]). This finding implies that the YqiI protein and the other proteins encoded by this gene cluster, the lipoprotein YqiH and the cytoplasmic glycerophosphodiester phosphodiesterase YqiK, serve a physiological function in cells that are continuously exposed to extremes in salinity. However, none of the *yqiHIK*-encoded proteins are essential for the growth of *B. subtilis* under these challenging conditions ([Fig. 4A] and [B]).

We observed striking morphological changes during the phase of acclimation of *B. subtilis* to sustained high salinity ([Fig. 4C]). During this stage, the morphology of the cells is very diverse, with the appearance of twisted and curved forms and
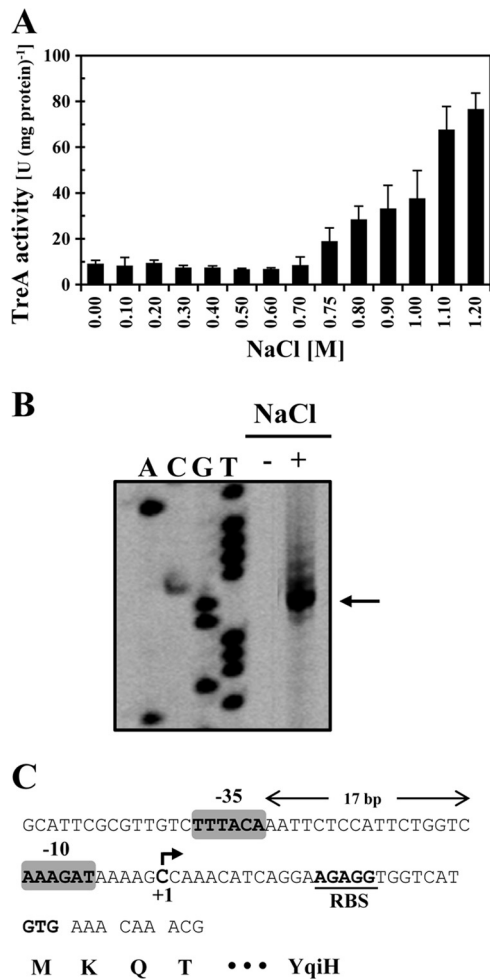
A

B

C

FIG 7 Osmotic regulation of *yqiH-treA* expression and identification of the *yqiHIK* transcription start site by primer extension analysis. (A) Determination of TreA activity in cells of strain KFB15 (*yqiH-treA*) cultured in SMM with increasing NaCl concentrations. All cell samples were harvested for TreA enzyme activity measurements at the mid-exponential growth phase (OD_{578} of about 1.0 to 1.5). (B) Primer extension analysis of the *yqiHIK* transcript in cells of *B. subtilis* strain 168 carrying plasmid pKF16 (*yqiH'*) cultured either in SMM (−) or in SMM with 1.2 M NaCl (+). (C) Nucleotide sequence of the *yqiHIK* promoter region. The transcription initiation site (+1) is indicated by a bent arrow. The −35 and −10 regions are highlighted with gray boxes and are separated by 17 bp. The ribosome-binding site (RBS) of the *yqiH* gene, its start codon, and the N-terminal amino acid sequence of the YqiH protein are shown.

the appearance of bulges at the cell poles (Fig. 4C and 5C). Since the murein sacculus determines cell shape (61, 63), these observations imply underlying deformations in the architecture of the peptidoglycan (22, 66). Remarkably, microscopic observations of cells that have fully adjusted to sustained high-osmolarity surroundings revealed a normal rod-shaped appearance (Fig. 4C). Consequently, either the *B. subtilis* cell can actively remodel its murein sacculus to remove the deformations in cell wall architecture that it experiences during the process of acclimatization to high-salinity environments or all the misshaped cells have lysed by the time the osmotically challenged culture has entered the exponential growth phase. Assuming that the observed prominent cellular deformations are

reversible, the involvement of an amidase activity seems likely. However, the YqiI amidase is definitely not critical for such a process (Fig. 4C), and neither are the LytC, CwlC, CwlD, and YrvJ amidases (Fig. 4C). The fact that we were able to a construct a quintuple mutant lacking all of these amidases possessing an amidase_3 domain (PF015020) indicates that other types of amidases must be present in *B. subtilis*. Indeed, Smith et al. (55) pointed to a set of amidases (XlyA, XlyB, BlyA, CwlA, and CwlH) that are encoded by prophages or prophage-related DNA elements present in the *B. subtilis* genome. All these proteins are predicted to carry an amidase_2 domain (PF01510) (49), a domain which is frequently found in zinc-containing enzymes possessing *N*-acetylmuramoyl-L-alanine activity (36).

Our *yqiH-treA* reporter gene fusion studies revealed a pattern of osmotic control of gene expression in *B. subtilis* that has not been observed before, e.g., for the *proHJ* and *opuE* genes. The latter genes encode enzymes for the osmoadaptive synthesis of the compatible solute proline (8) and a transporter for its uptake from the medium (64), respectively, and their expression levels increase linearly in tune with the degree of the imposed osmotic stress. In contrast, the transcription of the *yqiHIK* operon remained at a basal level until the salinity of the growth medium exceeded a threshold concentration of 0.7 M NaCl (Fig. 7A), a level of salinity which constitutes a considerable degree of osmotic stress for the *B. subtilis* cell (4). How the *B. subtilis* cell manages to produce different output responses in terms of the pattern of *yqiHIK*, *proHJ*, and *opuE* transcription when it is challenged with the same environmental cue is currently unknown. This might depend on the particular sequence of a given promoter, its flanking DNA regions, and solute-catalyzed interactions (e.g., via K$^+$-glutamate) of the RNA polymerase with the promoter region (18, 33, 45). The *yqiHIK* promoter loses its osmotic control when it is mutationally converted to a promoter that perfectly matches the −10 and −35 consensus sequences of *B. subtilis* SigA-type promoters (Table 2). Hence, the deviations from the consensus sequence (24, 65) serve to keep the level of activity of this promoter low under non-salt-stress growth conditions (Table 2).

One of the most interesting findings of our study was the discovery of a 53-bp highly AT-rich region whose 5′ end is located 180 bp upstream of the −35 sequence of the *yqiHIK* promoter (Fig. 6A). Its integrity is critical for the functioning of the *yqiHIK* promoter (Fig. 6B) in response to the signal(s) that is otherwise gathered by *B. subtilis* during growth in high-salinity media. We can currently only speculate on possible molecular mechanisms that might underlie this phenomenon of osmoregulation and the control of promoter activity at a distance. The AT-rich region could possibly drive structural transitions in the DNA of the *yqiHIK* regulatory region to favor the interaction of the RNA polymerase with the promoter sequence in cells exposed to high-salinity environments, or it could be the target of a regulatory protein that promotes such interactions.

The 300-bp DNA regulatory region of the *yqiHIK* operon that we have identified in this study carries all sequences required in *cis* for the osmotic control of gene expression (Fig. 6 and 7). Thus, the *yqiHIK* promoter might serve in future studies as an interesting system for the genetic exploration of the sensing and signaling events that allow *B. subtilis* to detect an increase in the external

TABLE 2 Mutational analysis of the SigA-type promoter of the *yqiHIK* operon[a]

| Strain[b] | Plasmid[b] | *yqiHIK* promoter sequence[c] | | | Mean TreA activity (U mg protein^{-1}) ± SD | | Induction ratio |
		−35	−16	−10	0 M NaCl	1.2 M NaCl	
Consensus sequence		**TTGACA**	**TG**	**TATAAT**			
KFB15	pKF13	TTTACA	GT	AAAGAT	5 ± 1	49 ± 7	9.8
KFB33	pKF25	TTTACA	GT	AAAGA**G**	3 ± 1	3 ± 1	1.0
KFB24	pKF18	TT**G**ACA	GT	AAAGAT	7 ± 1	81 ± 11	11.6
KFB26	pKF20	TTTACA	GT	AAA**A**AT	5 ± 1	91 ± 3	18.2
KFB32	pKF24	TTTACA	GT	**T**ATA**A**T	230 ± 11	399 ± 21	1.7
KFB34	pKF26	TT**G**ACA	GT	**T**ATA**A**T	304 ± 3	429 ± 27	1.4
KFB25	pKF19	TTTACA	**TG**	AAAGAT	20 ± 8	286 ± 8	14.3
KFB35	pKF27	TT**G**ACA	**TG**	**T**ATA**A**T	264 ± 20	314 ± 2	1.2

[a] The promoter of the *yqiHIK* operon was altered stepwise by site-directed mutagenesis to better fit the consensus sequence of SigA-type promoters. The introduced alterations in the −35, −16, and −10 regions are marked in boldface type. The cultures of the corresponding *yqiH-treA* reporter fusion strains were grown to the early exponential growth phase (OD$_{578}$ of about 1 to 1.5) either in SMM or in SMM containing 1.2 M NaCl and assayed for TreA enzyme activity.
[b] The designation of *yqiH-treA* fusion plasmid carrying the indicated mutations in the promoter region is given. These plasmids were used to recombine the mutant *yqiH-treA* reporter gene fusions as a single copy into the *amyE* gene, and the designations of the resulting strains are given.
[c] The consensus sequences of SigA-type promoters (24, 65) at their −10, −16, and −35 regions are shown. Strain KFB16 carries the *yqiH-treA* reporter fusion with the wild-type *yqiHIK* promoter sequence.

osmolarity and physiologically cope with this environmental challenge through targeted gene expression in a timely manner.

REFERENCES

1. **Albano M, et al.** 2005. The Rok protein of *Bacillus subtilis* represses genes for cell surface and extracellular functions. J. Bacteriol. **187**:2010–2919.
2. **Arnold K, Bordoli L, Kopp J, Schwede T.** 2006. The SWISS-MODEL workspace: a Web-based environment for protein structure homology modelling. Bioinformatics **22**:195–201.
3. **Barbe V, et al.** 2009. From a consortium sequence to a unified sequence: the *Bacillus subtilis* 168 reference genome a decade later. Microbiology **155**:1758–1775.
4. **Boch J, Kempf B, Bremer E.** 1994. Osmoregulation in *Bacillus subtilis*: synthesis of the osmoprotectant glycine betaine from exogenously provided choline. J. Bacteriol. **176**:5364–5371.
5. **Booth IR, Edwards MD, Black S, Schumann U, Miller S.** 2007. Mechanosensitive channels in bacteria: signs of closure? Nat. Rev. Microbiol. **5**:431–440.
6. **Bremer E.** 2002. Adaptation to changing osmolarity, p 385–391. *In* Sonenshein AL, Hoch JA, Losick R (ed), *Bacillus subtilis* and its closest relatives. ASM Press, Washington, DC.
7. **Bremer E, Krämer R.** 2000. Coping with osmotic challenges: osmoregulation through accumulation and release of compatible solutes, p 79–97.
8. *In* Storz G, Hengge-Aronis R (ed), Bacterial stress responses. ASM Press, Washington, DC.
8. **Brill J, Hoffmann T, Bleisteiner M, Bremer E.** 2011. Osmotically controlled synthesis of the compatible solute proline is critical for cellular defense of *Bacillus subtilis* against high osmolarity. J. Bacteriol. **193**:5335–5346.
9. **Brückner R.** 1992. A series of shuttle vectors for *Bacillus subtilis* and *Escherichia coli*. Gene **122**:187–192.
10. **Claessen D, et al.** 2008. Control of the cell elongation-division cycle by shuttling of PBP1 protein in *Bacillus subtilis*. Mol. Microbiol. **68**:1029–1046.
11. **Cutting SM, Vander Horn PB.** 1990. Genetic analysis, p 27–74. *In* Harwood CR, Cutting SM (ed), Molecular biological methods for *Bacillus*. John Wiley & Sons, Inc, Chichester, United Kingdom.
12. **Dorman CJ.** 2009. Nucleoid-associated proteins and bacterial physiology. Adv. Appl. Microbiol. **67**:47–64.
13. **Dorman CJ, Corcoran CP.** 2009. Bacterial DNA topology and infectious disease. Nucleic Acids Res. **37**:672–678.
14. **Eiamphungporn W, Helmann JD.** 2009. Extracytoplasmic function sigma factors regulate expression of the *Bacillus subtilis* yabE gene via a *cis*-acting antisense RNA. J. Bacteriol. **191**:1101–1105.
15. **Firczuk M, Bochtler M.** 2007. Folds and activities of peptidoglycan amidases. FEMS Microbiol. Rev. **31**:676–691.
16. **Foster SJ.** 1991. Cloning, expression, sequence analysis and biochemical characterization of an autolytic amidase of *Bacillus subtilis* 168 trpC2. J. Gen. Microbiol. **137**:1987–1998.
17. **Gotsche S, Dahl MK.** 1995. Purification and characterization of the phospho-alpha-(1,1)-glucosidase (TreA) of *Bacillus subtilis* 168. J. Bacteriol. **177**:2721–2726.
18. **Gralla JD, Vargas DR.** 2006. Potassium glutamate as a transcriptional inhibitor during bacterial osmoregulation. EMBO J. **25**:1515–1521.
19. **Guerout-Fleury AM, Frandsen N, Stragier P.** 1996. Plasmids for ectopic integration in *Bacillus subtilis*. Gene **180**:57–61.
20. **Hahne H, et al.** 2010. A comprehensive proteomics and transcriptomics analysis of *Bacillus subtilis* salt stress adaptation. J. Bacteriol. **192**:870–882.
21. **Harwood CR, Archibald AR.** 1990. Growth, maintenance and general techniques, p 1–26. *In* Harwood CR, Cutting SM (ed), Molecular biological methods for *Bacillus*. John Wiley & Sons, Inc, Chichester, United Kingdom.
22. **Hayhurst EJ, Kailas L, Hobbs JK, Foster SJ.** 2008. Cell wall peptidoglycan architecture in *Bacillus subtilis*. Proc. Natl. Acad. Sci. U. S. A. **105**:14603–14608.
23. **Helfert C, Gotsche S, Dahl MK.** 1995. Cleavage of trehalose-phosphate in *Bacillus subtilis* is catalysed by a phospho-alpha-(1-1)-glucosidase encoded by the *treA* gene. Mol. Microbiol. **16**:111–120.
24. **Helmann JD.** 1995. Compilation and analysis of *Bacillus subtilis* sigma A-dependent promoter sequences: evidence for extended contact between

RNA polymerase and upstream promoter DNA. Nucleic Acids Res. **23:** 2351–2360.

25. **Herzberg C, et al.** 2007. SPINE: a method for the rapid detection and analysis of protein-protein interactions *in vivo*. Proteomics **7:**4032–4035.

26. **Höltje JV.** 1998. Growth of the stress-bearing and shape-maintaining murein sacculus of *Escherichia coli*. Microbiol. Mol. Biol. Rev. **62:**181–203.

27. **Höper D, Bernhardt J, Hecker M.** 2006. Salt stress adaptation of *Bacillus subtilis*: a physiological proteomics approach. Proteomics **6:**1550–1562.

28. **Höper D, Völker U, Hecker M.** 2005. Comprehensive characterization of the contribution of individual SigB-dependent general stress genes to stress resistance of *Bacillus subtilis*. J. Bacteriol. **187:**2810–2826.

29. **Ishikawa S, Kawahara S, Sekiguchi J.** 1999. Cloning and expression of two autolysin genes, *cwIU* and *cwIV*, which are tandemly arranged on the chromosome of *Bacillus polymyxa* var. *colistinus*. Mol. Gen. Genet. **262:** 738–748.

30. **Jiang H, Si F, Margolin W, Sun SX.** 2011. Mechanical control of bacterial cell shape. Biophys. J. **101:**327–335.

31. **Kawai Y, et al.** 2011. A widespread family of bacterial cell wall assembly proteins. EMBO J. **30:**4931–4941.

32. **Kempf B, Bremer E.** 1998. Uptake and synthesis of compatible solutes as microbial stress responses to high osmolality environments. Arch. Microbiol. **170:**319–330.

33. **Kontur WS, Capp MW, Gries TJ, Saecker RM, Record MT, Jr.** 2010. Probing DNA binding, DNA opening, and assembly of a downstream clamp/jaw in *Escherichia coli* RNA polymerase-lambdaP(R) promoter complexes using salt and the physiological anion glutamate. Biochemistry **49:**4361–4373.

34. **Kuroda A, Sekiguchi J.** 1991. Molecular cloning and sequencing of a major *Bacillus subtilis* autolysin gene. J. Bacteriol. **173:**7304–7312.

35. **Kuwayama H, et al.** 2002. PCR-mediated generation of a gene disruption construct without the use of DNA ligase and plasmid vectors. Nucleic Acids Res. **30:**E2. doi:10.1093/nar/30.2.e2.

36. **Layec S, Decaris B, Leblond-Bourget N.** 2008. Diversity of Firmicutes peptidoglycan hydrolases and specificities of those involved in daughter cell separation. Res. Microbiol. **159:**507–515.

37. **Lazarevic V, Margot P, Soldo B, Karamata D.** 1992. Sequencing and analysis of the *Bacillus subtilis lytRABC* divergon: a regulatory unit encompassing the structural genes of the N-acetylmuramoyl-L-alanine amidase and its modifier. J. Gen. Microbiol. **138:**1949–1961.

38. **Letunic I, Doerks T, Bork P.** 2012. SMART 7: recent updates to the protein domain annotation resource. Nucleic Acids Res. **40:**D302–D305. doi:10.1093/nar/gkr931.

39. **Lopez CS, et al.** 2000. Biochemical and biophysical studies of *Bacillus subtilis* envelopes under hyperosmotic stress. Int. J. Food Microbiol. **55:** 137–142.

40. **Lopez CS, Heras H, Ruzal SM, Sanchez-Rivas C, Rivas EA.** 1998. Variations of the envelope composition of *Bacillus subtilis* during growth in hyperosmotic medium. Curr. Microbiol. **36:**55–61.

41. **Lucht JM, Dersch P, Kempf B, Bremer E.** 1994. Interactions of the nucleoid-associated DNA-binding protein H-NS with the regulatory region of the osmotically controlled *proU* operon of *Escherichia coli*. J. Biol. Chem. **269:**6578–6586.

42. **Margot P, Pagni M, Karamata D.** 1999. *Bacillus subtilis* 168 gene *lytF* encodes a gamma-D-glutamate-meso-diaminopimelate muropeptidase expressed by the alternative vegetative sigma factor, sigma D. Microbiology **145:**57–65.

43. **Miller JH.** 1972. Experiments in molecular genetics. Cold Spring Harbor Laboratory, Cold Spring Harbor, NY.

44. **Mishima M, et al.** 2005. Solution structure of the peptidoglycan binding domain of *Bacillus subtilis* cell wall lytic enzyme CwlC: characterization of the sporulation-related repeats by NMR. Biochemistry **44:**10153–10163.

45. **Nagarajavel V, Madhusudan S, Dole S, Rahmouni AR, Schnetz K.** 2007. Repression by binding of H-NS within the transcription unit. J. Biol. Chem. **282:**23622–23630.

46. **Nicolas P, et al.** 2012. Condition-dependent transcriptome reveals high-level regulatory architecture in *Bacillus subtilis*. Science **335:**1103–1106.

47. **Palomino MM, Sanchez-Rivas C, Ruzal SM.** 2009. High salt stress in *Bacillus subtilis*: involvement of PBP4* as a peptidoglycan hydrolase. Res. Microbiol. **160:**117–124.

48. **Pittelkow M, Tschapek B, Smits SH, Schmitt L, Bremer E.** 2011. The crystal structure of the substrate-binding protein OpuBC from *Bacillus subtilis* in complex with choline. J. Mol. Biol. **411:**53–67.

49. **Punta M, et al.** 2012. The Pfam protein families database. Nucleic Acids Res. **40:**D290–D301. doi:10.1093/nar/gkr1065.

50. **Reddick JJ, Williams JK.** 2008. The *mmgA* gene from *Bacillus subtilis* encodes a degradative acetoacetyl-CoA thiolase. Biotechnol. Lett. **30:** 1045–1050.

51. **Sambrook J, Fritsch EF, Maniatis T.** 1989. Molecular cloning: a laboratory manual, 2nd ed. Cold Spring Harbor Laboratory, Cold Spring Harbor, NY.

52. **Sekiguchi J, et al.** 1995. Nucleotide sequence and regulation of a new putative cell wall hydrolase gene, *cwlD*, which affects germination in *Bacillus subtilis*. J. Bacteriol. **177:**5582–5589.

53. **Shah IM, Dworkin J.** 2010. Induction and regulation of a secreted peptidoglycan hydrolase by a membrane Ser/Thr kinase that detects muropeptides. Mol. Microbiol. **75:**1232–1243.

54. **Shida T, Hattori H, Ise F, Sekiguchi J.** 2001. Mutational analysis of catalytic sites of the cell wall lytic N-acetylmuramoyl-L-alanine amidases CwlC and CwlV. J. Biol. Chem. **276:**28140–28146.

55. **Smith TJ, Blackman SA, Foster SJ.** 2000. Autolysins of *Bacillus subtilis*: multiple enzymes with multiple functions. Microbiology **146:**249–262.

56. **Smits WK, Grossman AD.** 2010. The transcriptional regulator Rok binds A+T-rich DNA and is involved in repression of a mobile genetic element in *Bacillus subtilis*. PLoS Genet. **6:**e1001207. doi:10.1371/journal.pgen.1001207.

57. **Spiegelhalter F, Bremer E.** 1998. Osmoregulation of the *opuE* proline transport gene from *Bacillus subtilis*: contributions of the sigma A- and sigma B-dependent stress-responsive promoters. Mol. Microbiol. **29:**285–296.

58. **Steil L, Hoffmann T, Budde I, Völker U, Bremer E.** 2003. Genome-wide transcriptional profiling analysis of adaptation of *Bacillus subtilis* to high salinity. J. Bacteriol. **185:**6358–6370.

59. **Thompson JD, Plewniak F, Thierry JC, Poch O.** 2000. DbClustal: rapid and reliable global multiple alignments of protein sequences detected by database searches. Nucleic Acids Res. **28:**2919–2926.

60. **Tjalsma H, et al.** 2004. Proteomics of protein secretion by *Bacillus subtilis*: separating the "secrets" of the secretome. Microbiol. Mol. Biol. Rev. **68:** 207–233.

61. **Vollmer W, Blanot D, de Pedro MA.** 2008. Peptidoglycan structure and architecture. FEMS Microbiol. Rev. **32:**149–167.

62. **Vollmer W, Joris B, Charlier P, Foster S.** 2008. Bacterial peptidoglycan (murein) hydrolases. FEMS Microbiol. Rev. **32:**259–286.

63. **Vollmer W, Seligman SJ.** 2010. Architecture of peptidoglycan: more data and more models. Trends Microbiol. **18:**59–66.

64. **von Blohn C, Kempf B, Kappes RM, Bremer E.** 1997. Osmostress response in *Bacillus subtilis*: characterization of a proline uptake system (OpuE) regulated by high osmolarity and the alternative transcription factor sigma B. Mol. Microbiol. **25:**175–187.

65. **Voskuil MI, Chambliss GH.** 1998. The −16 region of *Bacillus subtilis* and other gram-positive bacterial promoters. Nucleic Acids Res. **26:**3584–3590.

66. **Wang S, Furchtgott L, Huang KC, Shaevitz JW.** 2012. Helical insertion of peptidoglycan produces chiral ordering of the bacterial cell wall. Proc. Natl. Acad. Sci. U. S. A. **109:**E595–604.

67. **Whatmore AM, Reed RH.** 1990. Determination of turgor pressure in *Bacillus subtilis*: a possible role for K+ in turgor regulation. J. Gen. Microbiol. **136:**2521–2526.

68. **Wood JM.** 2011. Bacterial osmoregulation: a paradigm for the study of cellular homeostasis. Annu. Rev. Microbiol. **65:**215–238.

69. **Wood JM, et al.** 2001. Osmosensing and osmoregulatory compatible solute accumulation by bacteria. Comp. Biochem. Physiol. A Mol. Integr. Physiol. **130:**437–460.

70. **Yamamoto H, Kurosawa S, Sekiguchi J.** 2003. Localization of the vegetative cell wall hydrolases LytC, LytE, and LytF on the *Bacillus subtilis* cell surface and stability of these enzymes to cell wall-bound or extracellular proteases. J. Bacteriol. **185:**6666–6677.